GC-MS PHYTOCHEMICAL ANALYSIS AND COMPARATIVE PHOTOCATALYTIC DEGRADATION PROCEDURE BETWEEN ZNO AND SB_2O_3 IN EXTRACT OF LEAF *GYNANDRIRIS SISYRINCHIUM* (L.) PARL.

Huda J. M. Altameme[1] H Y. Al-gubury[2] M. A. Ismeel[3]
Prof. Assis. Prof. Assis. Prof.
[1] Dept. Biology, College of Science for Women, University of Babylon, Iraq.
[2,3] Dept. Chemistry, College of Science for Women, University of Babylon, Iraq.
wsci.huda.j@uobabylon.edu.iq, h.yahya40@yahoo.com

ABSTRACT

The present research was conducted to the *Gynandris sisyrinchium* (L.) Parl. leaves extract to identify the phytochemicals present and determine the qualitative presence of phenols and flavonoids. The GC-MS findings have different peaks to determine the existence of 23 phytochemical compounds which may have a role in pharmacological activities. On another side, A photocatalytic degradation of extracted dye using ZnO and Sb_2O_3 was tested, which is done by the photodegrade of a suspended aqueous solution of extracted dye with 0.17gm/100ml of semiconductor starting with ZnO then Sb_2O_3 under UV lamp (125 Watts) at 298 K. To reach the best photodegradation several experiments have been carried out. Started by the effect on the photocatalytic degradation of the extracted colorant of the semiconductor and the effect of the dye concentration extracted. Using UV-Vis spectrophotometer, the products were tested. It can be noted, from all experiments, that the employing of zinc oxide as a photocatalyst was found to be more effective than Sb_2O_3 to degradation of dye.

Keyword: Iridaceae, leaves extraction, coloring degradation, removal, antimony trioxide.

التحليل الكيميائي النباتي GC-MS وعملية التحلل الضوئي المقارن بين ZnO و Sb2O3 في مستخلص أوراق *Gynandriris sisyrinchium* (L.) Parl.

هدى جاسم محمد التميمي[1] حازم يحيى الجبوري[2] محمد عبد الرضا إسماعيل[3]
أستاذ استاذ مساعد استاذ مساعد
[1] قسم علوم الحياة ، كلية العلوم للبنات ، جامعة بابل ، الحلة ، العراق
[2و3] قسم الكيمياء، كلية العلوم للبنات، جامعة بابل، الحلة، العراق

المستخلص

تم إجراء البحث الحالي ل مستخلص أوراق *Gynandris sisyrinchium* (L.) Parl. للتعرف على المواد الكيميائية النباتية الموجودة وتحديد الوجود النوعي للمركبات الفينولية والفلافونيدات. واظهرت نتائج GC–MS وجود قمم مختلفة تحدد وجود 23 مركبًا كيميائيًا نباتيًا التي قد يكون لها دور في الفعاليات الدوائية.. من ناحية أخرى، تم اختبار التحلل التحفيزي الضوئي للصبغة المستخرجة باستخدام ZnO و Sb2O3، وتم بواسطة التحلل الضوئي لمحلول مائي معلق للصبغة المستخرجة باستخدام 0.17 جم / 100 مل من أشباه الموصلات بدءًا من ZnO ثم Sb2O3 تحت مصباح الأشعة فوق البنفسجية (125 واط) عند درجة حرارة 298 كلفن، تم إجراء العديد من التجارب للوصول إلى أفضل تدهور ضوئي. بدأ بالتأثير على التحلل التحفيزي الضوئي للملون المستخلص من أشباه الموصلات وتأثير تركيز الصبغة المستخرجة. باستخدام مقياس الطيف الضوئي UV–Vis، تم اختبار النواتج. وأمكن ملاحظة، من خلال جميع التجارب، أن استخدام أكسيد الزنك كمحفز ضوئي وجد أنه أكثر فعالية من Sb2O3 في تحلل الصبغة.

الكلمات الافتتاحية: العائلة السوسنية، مستخلص الاوراق، تكسير الالوان، الازالة، ثالث اوكسيد الانتيمون

Received:15/3/2021, Accepted:2/6/2021

INTRODUCTION

The Iridaceae family is one of the plant families planted for decorative purposes. Four genera reflect this family in Flora of Iraq (*Iris* L., *Gynandriris* Parl., *Crocus* L. and *Gladiolus* L.). The only plant in the *Gynandriris* genus widely grown in the desert area of Iraq is *Gynandriris sisyrinchium* (L.) Parl. (Syns. *Iris sisyrinchium* L., and *Moraea Sisyrinchium* (L.) Ker Gawl.) (19). The plant described as perennial herbs, bulbous, small to medium in size. Bulb globose or ovoid, flexible roots. Aerial stem short, simple or branched, circular section. Bifacial, coeval, canaliculate, subdivisional leaves; the basal 1 or 2. Inflorescence of cymose or corymbose aspect, sometimes with solitary flowers; bracts 1 or 2, membranous, Actinomorphic, erect, sub-sessile flowers. Perianth with 2 whorls of very different appearance, free tepals Equilateral stamens, opposed to external tepals; filaments filiform, stigma subapical, reduced to an inconspicuous, bilobed transverse lip, located on the abaxial surface of the stylar laminae, at the base of the crests. Fruit in capsule, loculicidal, trigone, with persistent beak, hidden between the bracts. Earlier phytochemicals analysis has shown that numerous secondary metabolites, including flavonoids, bioflavonoids, quinones, and xanthones, are present in *Gynandriris* (2), flavonoids such as apigenin, apigenin 7-*O*-β-glucopyranoside, luteolin 7-*O*-β-glucopyranoside, isovitexin, orientin, isoorientin and saponarin were isolated from the aerial part of *G.sisyrinchium* in Egypt (11). Another research in Jordan showed, 3,7,11,15-tetramethyl-2-hexadecen-1-ol, ledene oxide (II), furfural and trans-sabinol found to be the main components of the oil leaves, while phenylacetaldehyde, 8,9 dehydroneoisolongifolene , 8S,14-cedranediol and furfural were bulb's oil (7). In 2015, the last authors showed twelve compounds of methanol from *G.sisyrinchium* like (3′-methyl tenuifone; gynandrinone; β-sitosterol;7,3′-dimethoxy-5,6,4′-trihydroxyisoflavone,iristectorigenin; hispidulin; galangustin; 6-hydroxybiochanin A; ursolic acid; ladanetin; 4′-O-methylgenistein and β-sitosterol glucoside) and the antioxidant and cytotoxic functions described (6). The appearance of color in the water and drainage supplies is also the principal cause of environmental contamination for the health of humans and animals as a result of their toxicity and cancer (20,22). A high photocatalytic reaction process for isolated color photodegradation is the use of oxides of the metals, such as TiO2, ZnO and V2O5, in the photocatalytic degradation of certain biological containment. As a photocatalytic degradation of the extracted dye contaminants, an advanced oxidation mechanism (AOPs) known as photocatalysis has been used. The advanced method of oxidation is focused on the development of various active species, such as hydroxyl radicals (•OH), anion superoxide radicals (O2•-) to eliminate the contaminants of organic dyes.

MATERIALS AND METHODS

Preparation for plant extraction:

1- The aqueous extraction was carried out according to the method (13). During the time from March to June 2019, *G.sisyrinchium* leaves had been obtained from agricultural Babylon nurseries (Fig.1) which described the flora of Iraq based on morphological feature (10,19). For washing with tap water, the samples were transported at home for removing dust and insects, then 250 g floral parts were soaked in 500 ml of boiling water at 100° C at a room temperature of 48 hours with a continuous mix, allowing solubility of active substances in the solvent used. The extract was placed first in a soft cloth and then in filter paper Whatman No.1, the solvent was separated from the extract and then placed in the oven at 50° C. The powders were finally collected and then used for the analysis (8).

2-The methanolic extraction: According to (9), the methanolic extract was obtained, the leaves were air-dried and powdered. Then weighed and soaked 10 grams of powder for 3 days with 100 ml of methanol to dissolve the substances of different chemical components such as alkaloids and flavonoids (13). Then the extract is filtered and the residue removed

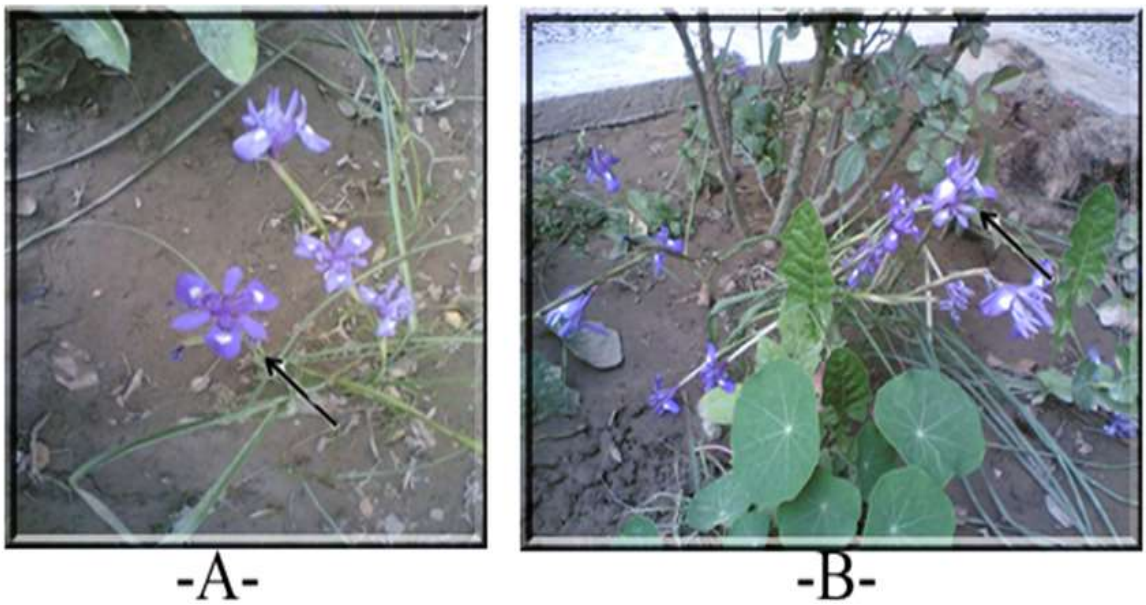

Fig. 1. (A, B) plant of *Gynandriris sisyrinchium*

GC-MS analytical phytochemical screening: Clarus 500 Perkin–Elmer (Auto Machine XL) attached to a Turbo-Gold–Perkin Elmer spectrometer 5.1 was used in GC-MS analysis with 2µl of methanol extraction from leaves *G.Sisyrinchium*. The GC/MS system has been provided with the Elite–1 column, made from 100% dimethylpolysiloxane and fused capillary silica (30m x 0.25mm diameter, 1 mm thick). Helium was the carrier gas at a 1.0 $ml.min^{-1}$ flowrate at a split ratio of 1:10, the temperature range is 110C° for 2min, rises 5C° min^{-1} to 200C° and is maintained at a 9min range, rises 5C° min^{-1} to 280C° and remains at a holding rate of 9min. The temperature of the injector and detector was held at 280 C^{o}. At 70 eV, mass spectra with a spectral range of 45-450 m/z were taken. Turbo-Mass Gold-Perkin Elmer and Turbo-Mass 5.2 were used for the mass detectors used in the research based on the manipulation of mass spectrums and Chromatograms (12). Most components were classified by mass spectrum and NIST library (14).

-Chemicals were used in photodegradation

1- Zinc oxide (ZnO): Has purity (99%), which given by Fluka AG.

2- Antimony trioxide (Sb_2O_3): was delivered by Fluka AG.

-Photo Procedure

The photocatalytic degradation process of dye was performed in the experimental equipment depicted in Fig.2. A horizontal cylindrical annular reactor consisting of two parts, in the external part water has been used for reaction solution cooling, A reaction vessel was the second part where the dye solution($100cm^3$) in the vessel was stirred by the magnetic stirrer to form of a suspension solution. A set of photocatalytic degradation of dye was performed using the UV light was positioned directly at the surface of the reactor vessel. At predetermined time intervals, $3cm^3$ of each reaction mixture was withdrawn and centrifuged, and the absorbance was determined at λmax of the dye by using UV-V is spectrophotometer.

Fig.2. The photocatalytic degradation cell was employed in the Photodegradation processes of extracted dye

RESULT AND DISCUSSION

Table 1 and Fig. 3 described and introduced the GC-MS methanol extract characterization of *G.sisyrinchium* leaves. twenty-three compounds have been classified as major chemical compounds. The first peak has been identified was Octan amide, N-(2-mercaptoethyl)- (Fig 4). The second highest level showed D-Glucose, 6-O-α-D-galactopyranosyl- (Fig. 5); The third highest peak was described 3-hydroxy-Dodecanoic acid (Fig.6) and followed with other compounds such as 9-Octadecenoic acid (Z)-, phenylmethyl ester(Benzyl oleate); Desulphosinigrin; 1H-Azonine , octahydro-1-nitroso-; 4H-Pyran-4-one , 2,3-dihydro-3,5-dihydroxy-6-methyl; 3-Trifluoroacetoxydodecane; 5,6-Dicarbadecaborane(12), 5,6-dimethyl-; 4-Hexenal , 6-hydroxy-4-methyl - , dimethyl acetal , acetate , (Z)-; Octanoic acid , 6-hydroxy-8-methoxy- , ε-lactone; 6-Acetyl-β-d-mannose; Estragole; α-D-Glucopyranoside ,O-α-D-glucopyranosyl (1.fwdarw.3)-ß-D-fructofuranosyl; 1-Hexadecanol , 2-methyl-; 4-(2,4,4-Trimethyl-cyclohexa-1,5-dienyl)-but-3-en-2-; I-Gala-l-ido-octonic lactone; 4-(1,5-Dihydroxy-2,6,6-trimethylcyclohex-2-enyl)but-3-en-2-one; Octahydrobenzo[b] pyran, 4a-acetoxy-5,5,8a-trimethy; 5,6,6-Trimethyl-5-(3-oxobut-1-enyl)-1-oxaspiro[2.5] octan-4-one; 7-Methyl-Z-tetradecen-1-ol acetate; 1-Hexadecanol , 2-methyl- and 3-Methyl –Z,Z-4,6-hexadecadiene (Fig 7-26).

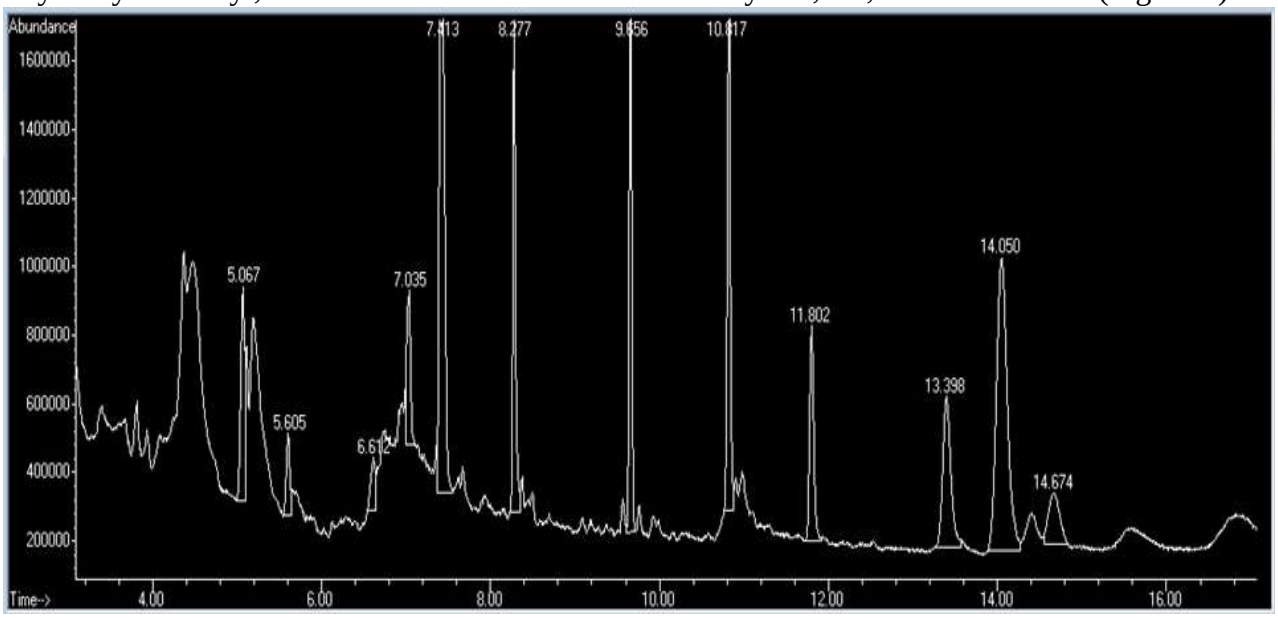

Fig.3. Crude methanolic extract mass spectrum of the *G.sisyrinchium* leaves

The Effect of catalyst masses on photocatalytic degradation of dye The influence of zinc oxide leaded mass and antimony trioxide mass respectively on Photocatalytic degradation dye was tested using 60 ppm of dye, at room temperature 298 K. As shown in Fig.27 the photodegradation processes of dye using masses of ZnO and Sb_2O_3 range (0.02 – 0.17 g/100cm^3) gradually increases with increasing of ZnO and Sb_2O_3 masses until reach to 0.17gm/100ml, then gradually decreases. When the loaded mass of catalyst equal 0.17gm/100ml the metal oxide ZnO and Sb_2O_3 can be supplied the highest absorption of UV light and as a sequence increase the degradation of dye. At the masses of catalyst higher than the optimum value of catalyst 0.17gm/100ml lead to decrease in the efficiency of photodegradation process due to the incident light has been reach to the first layers of extracted dye (2,3,15,16,17,18,21) At the mass of catalyst below the optimum value 0.17gm/100ml the surface area the of catalyst reduce therefor the rate of photodegradation of extracted dye decreased. It's clear From Fig.27 ZnO found to be more efficient than Sb_2O_3 because of an increase in the effective surface area. From Fig. 28 and 29 the percentage of photocatalytic degradation efficiency of ZnO equal to 88.80% while to Sb_2O_3 equal to 72.80%.

Table 1. The GC-MS investigation methanol extract from *G.sisyrinchium* leaves

Name of the compound	Retention time (min)	Molecular weight	Exact mass	Molecular formula	MS Fragment-Ions	Structure
Octanamide , N-(2-mercaptoethyl)-	3.110	203	203.134385	$C_{10}H_{21}NOS$	57,85,127,144,203	Figure 4
D-Glucose , 6-O-α-D-galactopyranosyl-	3.276	342	342.11621	$C_{12}H_{24}O_{12}$	60,73,110,212,261	Figure 5
3-hydroxy-Dodecanoic acid,	3.413	216	216.1725445	$C_{12}H_{24}O_3$	55,69,96,138,180	Figure 6
9-Octadecenoic acid (Z)-,phenylmethyl ester(Benzyl oleate)	3.808	372	372.30283	$C_{25}H_{40}O_2$	55,69,91,147,207,282	Figure 7
Desulphosinigrin	3.957	279	279.077658	$C_{10}H_{17}NO_6S$	60,73,85,127,145,213,262	Figure 8
1H-Azonine , octahydro-1-nitroso-	4.489	156	156.126264	$C_8H_{16}N_2O$	55,70,96,125,156	Figure 9
4H-Pyran-4-one, 2,3-dihydro-3,5-dihydroxy-6-methyl	5.221	144	144.042258	$C_6H_8O_4$	55,72,102,144	Figure 10
3-Trifluoroacetoxydodecane	5.599	282	282.180664	$C_{14}H_{25}F_3O_2$	55,69,83,97,111,140,168	Figure 11
5,6-Dicarbadecaborane(12), 5,6-dimethyl-	5.891	152	152.199644	$C_4H_{16}B_8$	113,147	Figure 12
4-Hexenal, 6-hydroxy-4-methyl -, dimethyl acetal, acetate, (Z)-	6.131	216	216.136159	$C_{11}H_{20}O_4$	58,75,93,110,152,184	Figure 13
Octanoic acid , 6-hydroxy-8-methoxy- , ε-lactone	6.423	172	172.109944		55,71,85,112,139,154	Figure 14
6-Acetyl-β-d-mannose	6.635	222	222.073953	$C_8H_{14}O_7$	60,97,126,144,165	Figure 15
Estragole	7.047	148	148.088815	$C_{10}H_{12}O$	51,63,77,91,121,148	Figure 16
α-D-Glucopyranoside, O-α-D-glucopyranosyl-(1.fwdarw.3)-ß-d-fruc	7.607	504	504.169035	$C_{18}H_{32}O_{16}$	60,73,85,97,126,145,193	Figure 17
1-Hexadecanol , 2-methyl-	8.305	256	256.276615	$C_{17}H_{36}O$	57,69,97,238	Figure 18
4-(2,4,4-Trimethyl-cyclohexa-1,5-dienyl)-but-3-en-2-	9.553	190	190.135765	$C_{13}H_{18}O$	77,91,119,147,157,175,190	Figure 19
I-Gala-l-ido-octonic lactone	9.770	238	238.068868	C8H14O8	73,112,189,238	Figure 20
4-(1,5-Dihydroxy-2,6,6-trimethylcyclohex-2-enyl)but-3-en-2-one	9.948	224	224.141245	$C_{13}H_{20}O_3$	55,69,81,91,109,135,163,181,224	Figure 21
Octahydrobenzo[b]pyran , 4a-acetoxy-5,5,8a-trimethy	10.880	240	240.1725445	$C_{14}H_{24}O_3$	55,69,97,111,124,137,151,165,180,197,240	Figure 22
5,6,6-Trimethyl-5-(3-oxobut-1-enyl)-1-oxaspiro[2.5] octan-4-one	11.000	236	236.141245	$C_{14}H_{20}O_3$	69,79,97,109,123,137,165,175,193,207,236	Figure 23
7-Methyl-Z-tetradecen-1-ol acetate	11.241	268	268.24023	$C_{17}H_{32}O_2$	55,81,99,239,263	Figure 24
1-Hexadecanol , 2-methyl-	13.404	256	256.276615	$C_{17}H_{36}O$	57,69,83,97,111,125,139,168,210,238,254	Figure 25
3-Methyl –Z,Z-4,6-hexadecadiene	14.102	236	236.2504015	$C_{17}H_{32}$	57,95,221	Figure 26

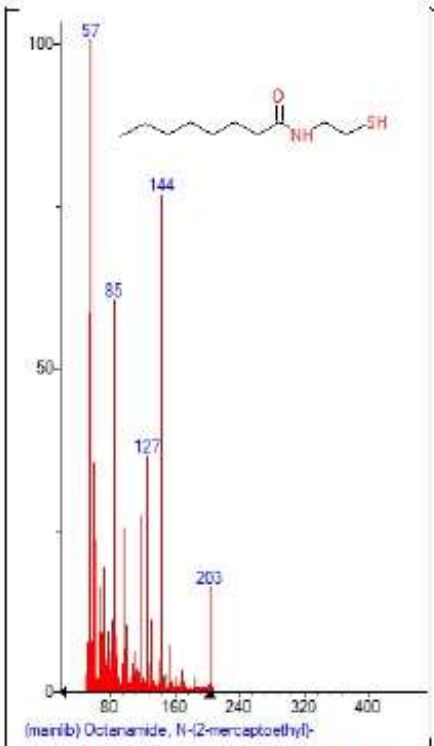

Figure 4: Chromatogram of Octanamide, N-(2-mercaptoethyl)-

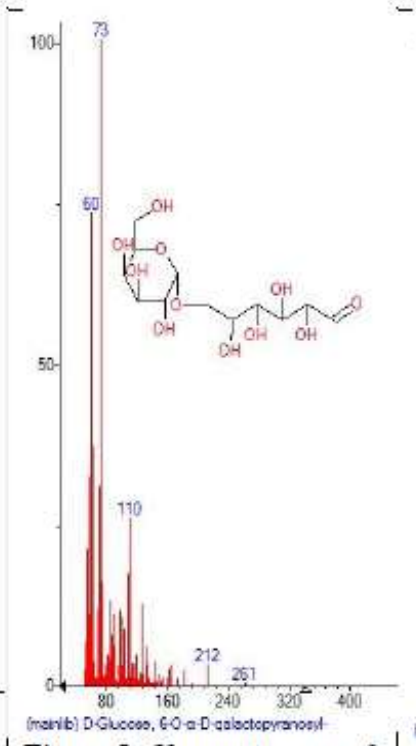

Figure 5: Chromatogram of D-Glucose, 6-O-α-D-galactopyranosyl-

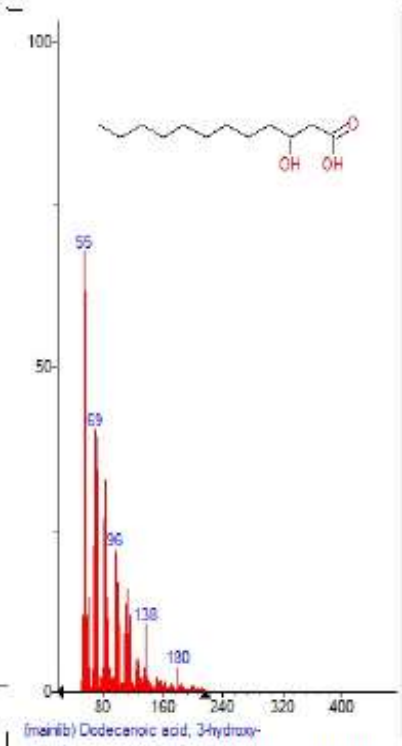

Figure 6: Chromatogram of 3-hydroxy-Dodecanoic acid,

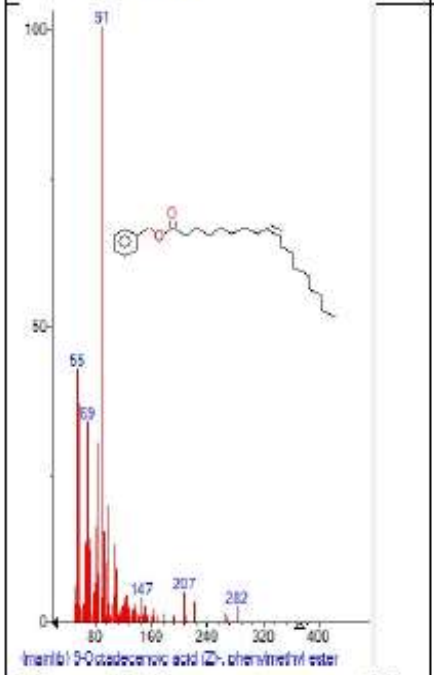

Figure 7: Chromatogram of 9-Octadecenoic acid (Z)-, phenylmethyl ester

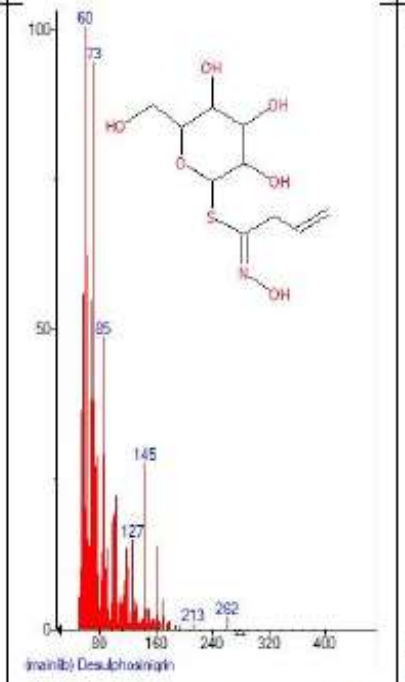

Figure 8: Chromatogram of Desulphosinigrin

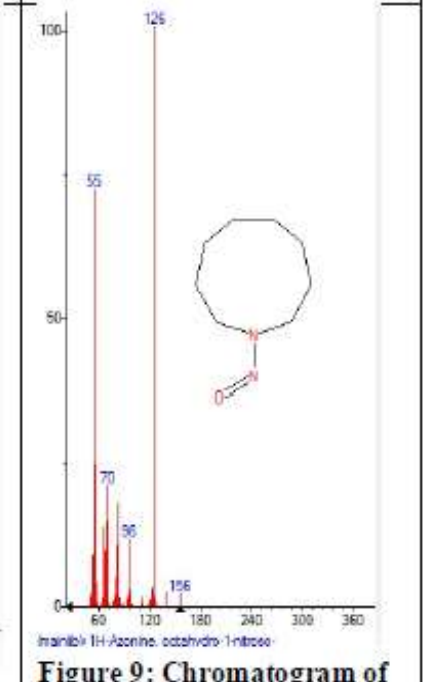

Figure 9: Chromatogram of 1H-Azonine, octahydro-1-nitroso-

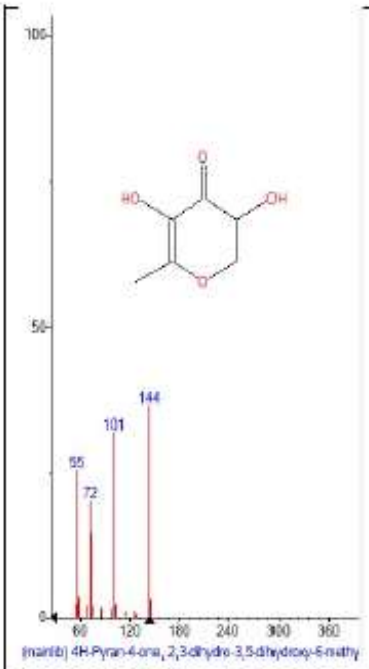

Figure 10: Chromatogram of 4H-Pyran-4-one , 2,3-dihydro-3,5-dihydroxy-6-methyl

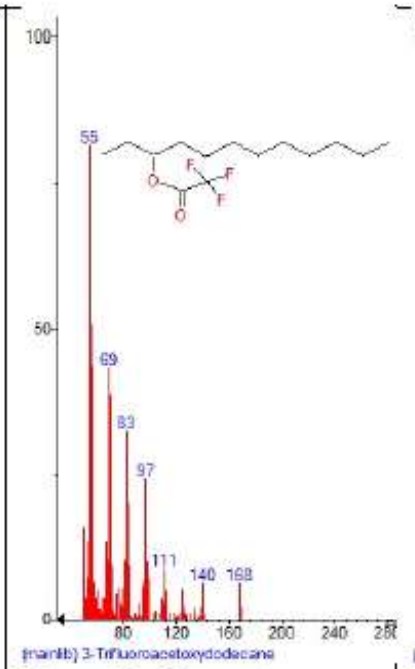

Figure 11: Chromatogram of 3-Trifluoroacetoxydodecane

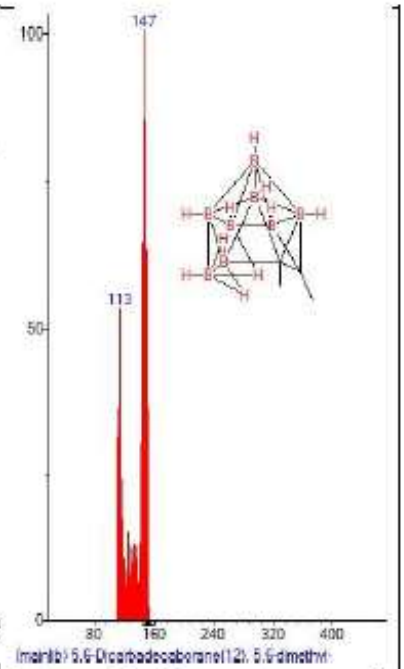

Figure 12: Chromatogram of 5,6-Dicarbadecaborane(12), 5,6-dimethyl-

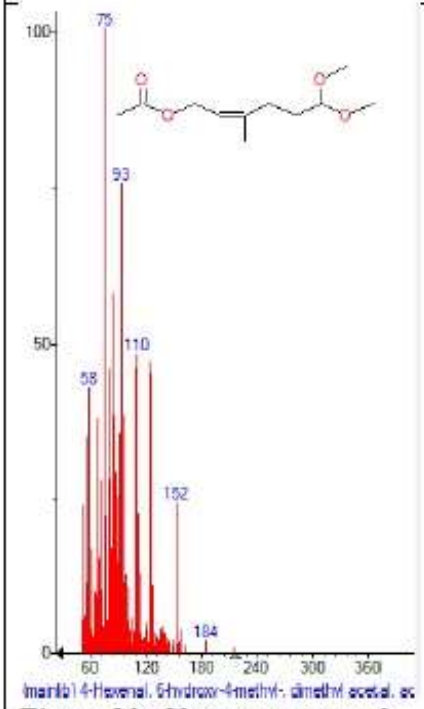

Figure 13: Chromatogram of 4-Hexenal, 6-hydroxy-4-methyl-, dimethyl acetal, acetate, (Z)-

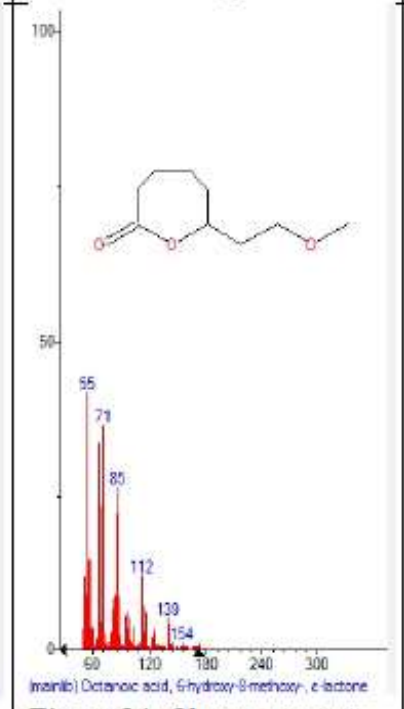

Figure 14: Chromatogram of Octanoic acid, 6-hydroxy-8-methoxy-, ε-lactone

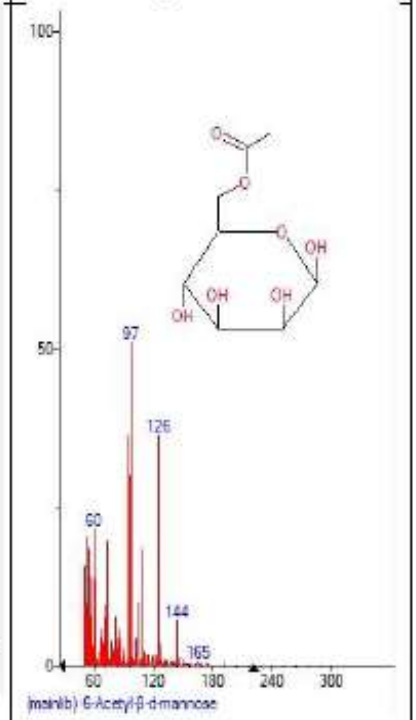

Figure 15: Chromatogram of 6-Acetyl-β-d-mannose

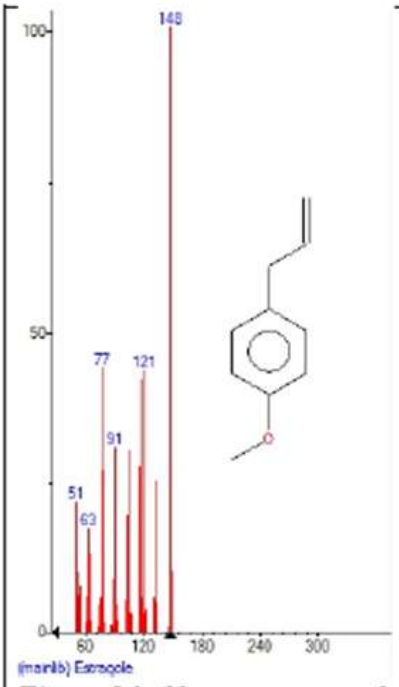

Figure 16: Chromatogram of Estragole

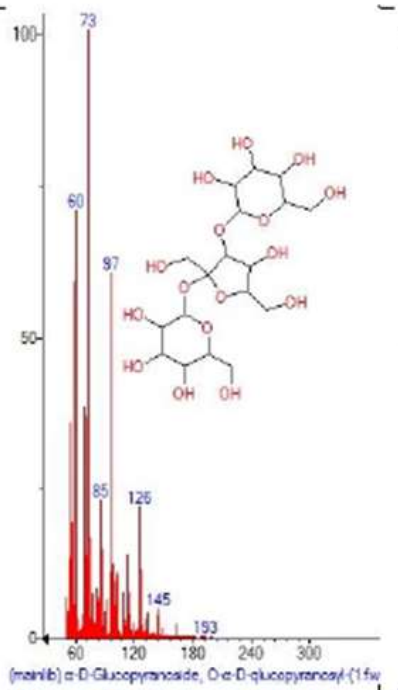

Figure 17: Chromatogram of α-D-Glucopyranoside, O-α-D-glucopyranosyl-(1.fwdarw.3)-ß-d-fruc

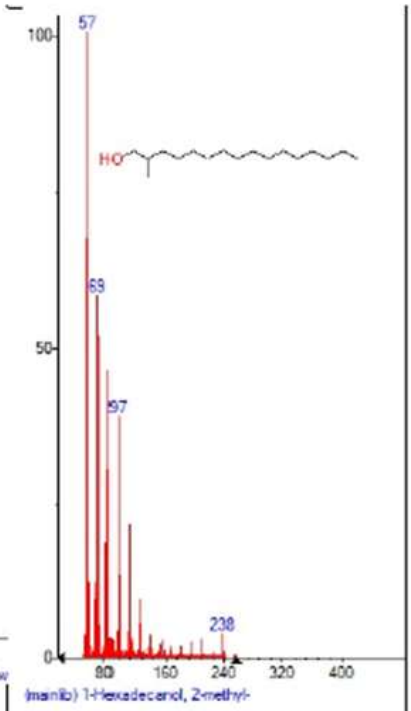

Figure 18: Chromatogram of 1-Hexadecanol, 2-methyl-

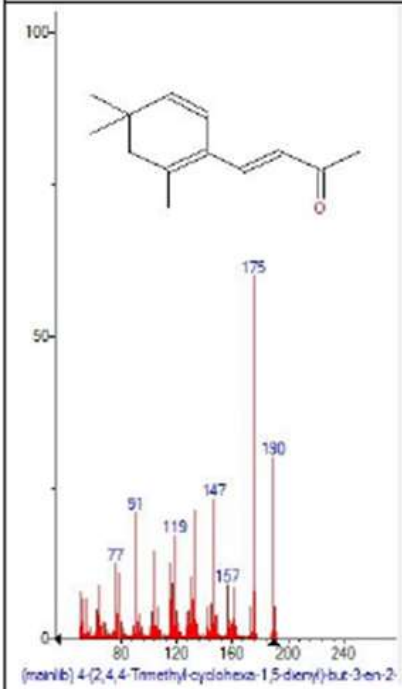

Figure 19: Chromatogram of 4-(2,4,4-Trimethyl-cyclohexa-1,5-dienyl)-but-3-en-2-

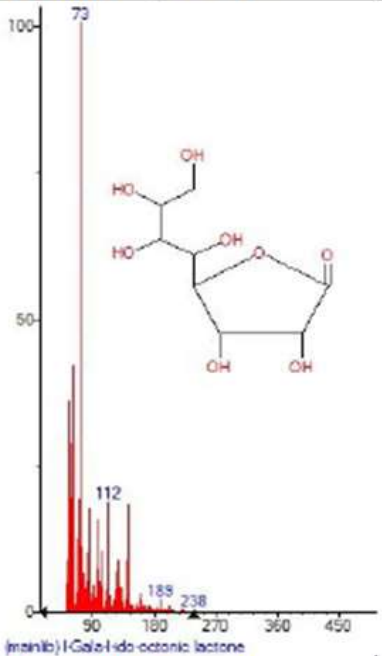

Figure 20: Chromatogram of I-Gala-I-ido-octonic lactone

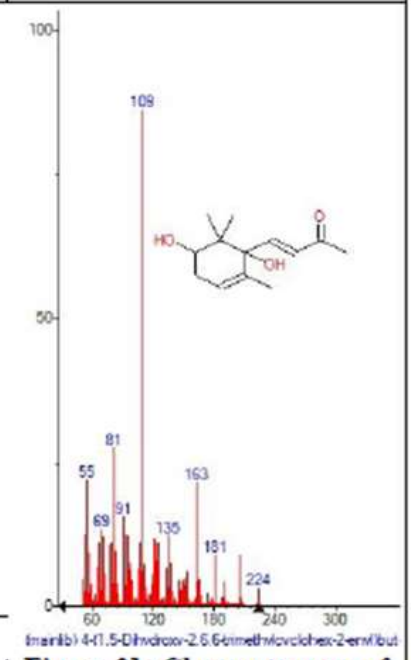

Figure 21: Chromatogram of 4-(1,5-Dihydroxy-2,6,6-trimethylcyclohex-2-enyl) but-3-en-2-one

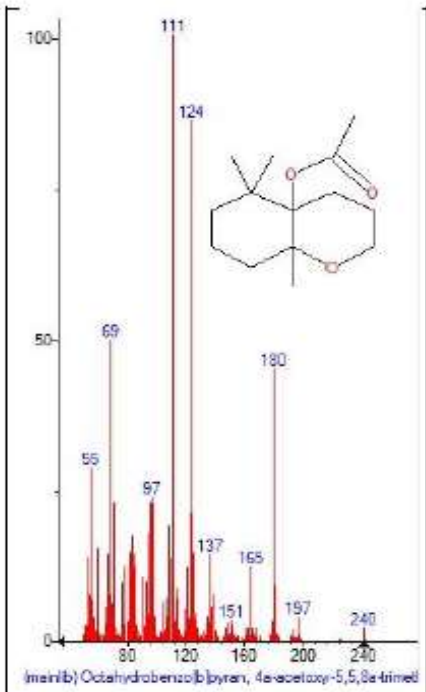

Figure 22: Chromatogram of Octahydrobenzo[b]pyran , 4a-acetoxy-5,5,8a-trimethy

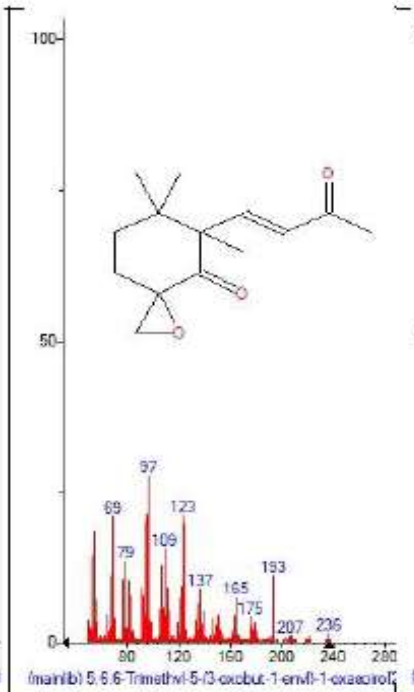

Figure 23: Chromatogram of 5,6,6-Trimethyl-5-(3-oxobut-1-enyl)-1-oxaspiro[2.5] octan-4-one

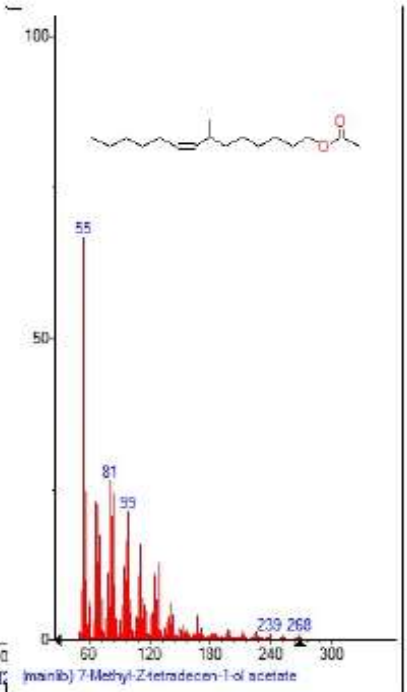

Figure 24: Chromatogram of 7-Methyl-Z-tetradecen-1-ol acetate

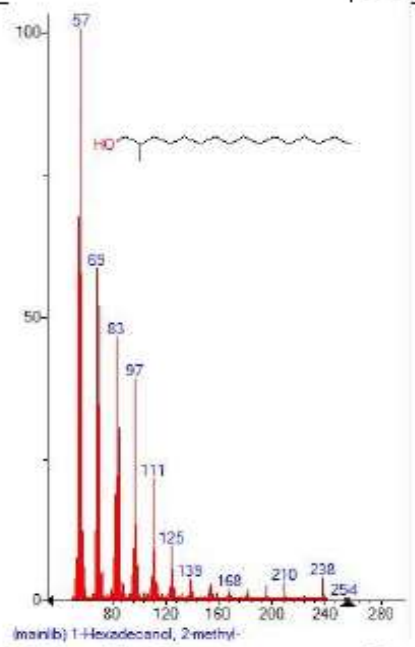

Figure 25: Chromatogram of 1-Hexadecanol, 2-methyl-

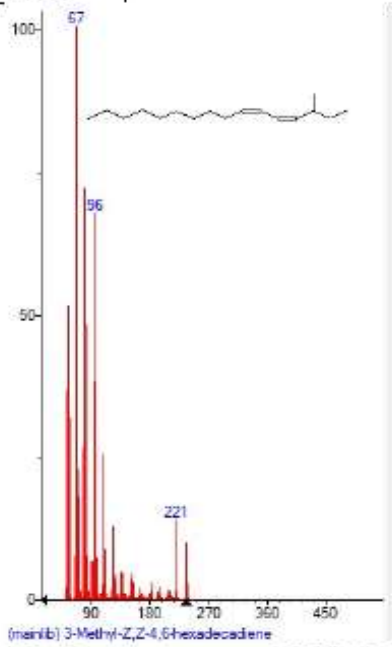

Figure 26: Chromatogram of 3-Methyl –Z, Z-4,6-hexadecadiene

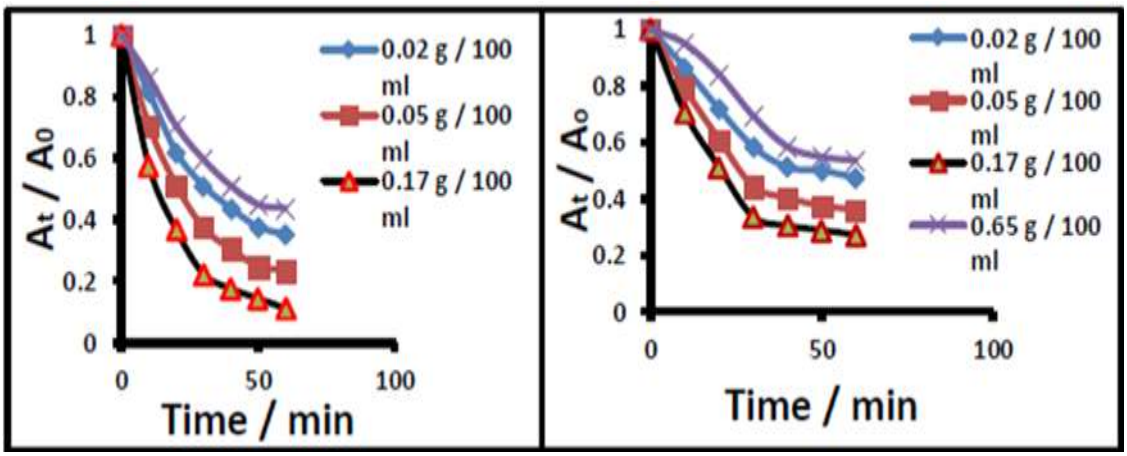

Fig.27. The change of (A_t /A_0) with exposure time at a concentration of extracted dye: a-for ZnO, b- for Sb_2O_3

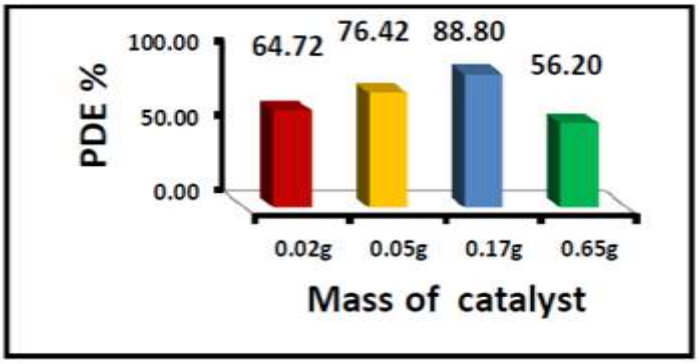

Fig.28. Photocatalytic degradation efficiency at different catalyst (ZnO) using 60 ppm of dye

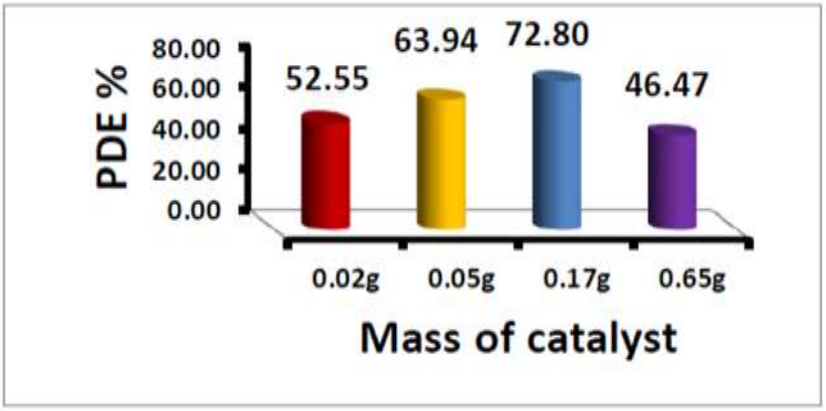

Fig.29. Photocatalytic degradation efficiency at different catalyst (Sb_2O_3) using 60 ppm of dye

The Effect of extracted dye concentration on photocatalytic degradation processes

A set of experiments was performed, to study the effect of the dye concentration range (60 – 90 ppm) on the degradation extracted dye using 0.17gm /100 ml, at 298 K. As shown in the Fig. 30. The rate degradation of extracted dye decreases with the increase of extracted dye. The concentration of extracted dye 60 ppm was the optimum value of dye to cover the suitable area of the catalyst particles, to absorbed exciting photons to activated metal oxide. After 60 mg/L of extracted dye the dye was act as internal filter to prevent the penetration of UV light through the inner layers of extracted dye on the catalyst surface (5). A shown in (Fig. 31 and 32) ZnO (90.40%) found to be more efficient than Sb_2O_3 (82.40 %).

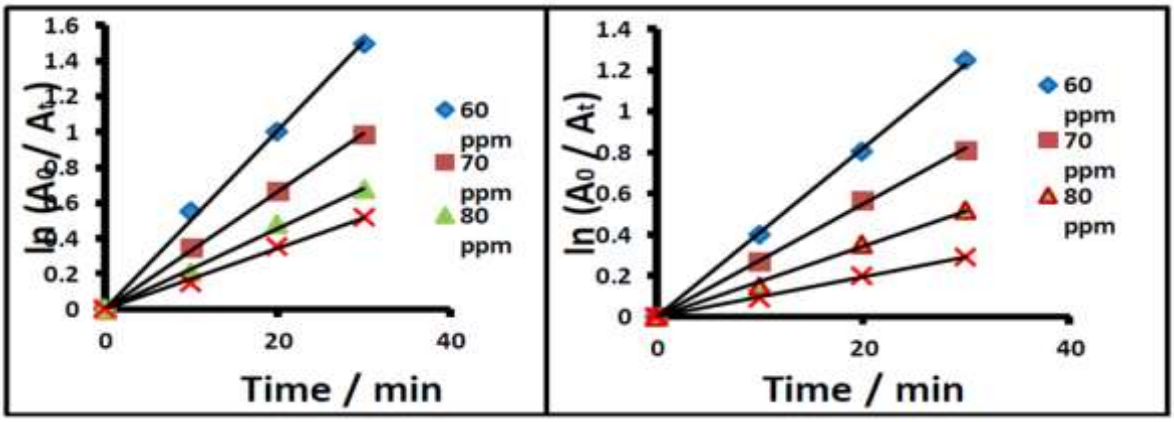

Fig.30. The change of (A / A0) with exposure time at the initial concentration of extracted dye: a-for ZnO, b- for Sb_2O_3

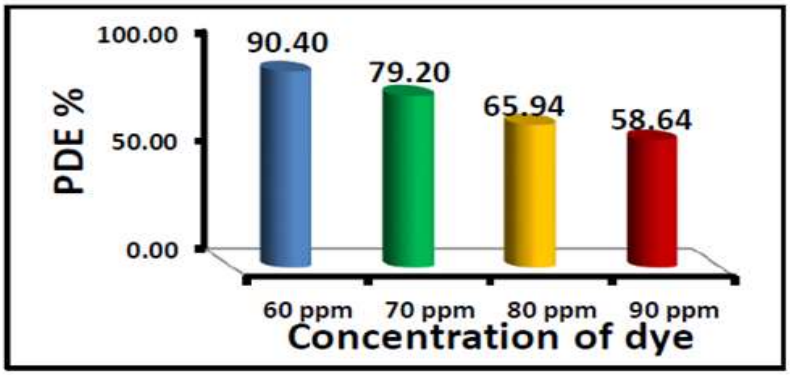

Fig. 31. Photocatalytic degradation efficiency at different catalyst (ZnO) using 60 ppm of extracted dye

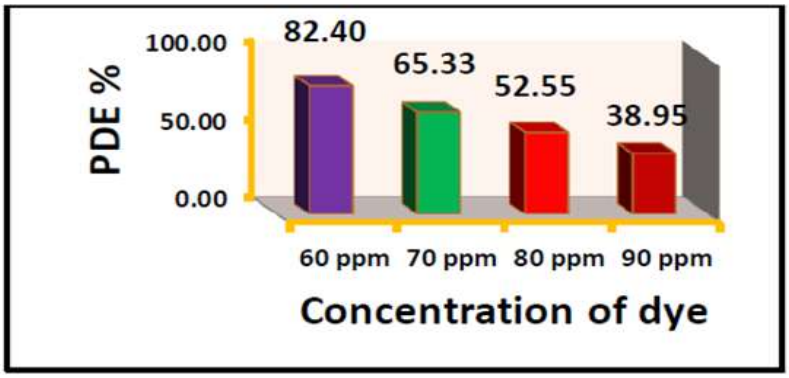

Fig. 32. Photocatalytic degradation efficiency at different catalyst (Sb_2O_3) using 60 ppm of extracted dye

The deterioration of extracted dye by 0.17g/100 ml catalyst was compared between ZnO and Sb2O3. It should be noted that in comparison with Sb2O3, ZnO had a higher photocatalytic activity which can be due to the increase of the effective surface of the catalyst leading to the increased photocatalytic activity for coloring degradation (4).

REFERENCES

1. Aburjai, T.; B.Amro; S. Al-Khalil; and D. Al-Eisawi. 2000. Acta Technologiae et Legis Medicamenti, 11(3): 137-145

2. Ahmed, M.A.; E. E. El-Katori and Z. H. Gharni. 2013**.** Photocatalytic degradation of methylene blue dye using Fe2O3/TiO2 nanoparticles prepared by sol–gel method, Journal of Alloys and Compounds, 553 (1) :19–29

3. Al-Gubury H. Y.; H. J. M. Altameme and M. M. Ali. 2018. Significant enhancement of photocatalytic activity of Zinc Oxide by extracted anthocyanin pigment and solar light. Plant Archives .18 (2):2723-2726

4. Algubury, H. Y. 2016. Study the activity of Titanium dioxide nanoparticle using orange G

dye, Malaysian Journal of Science 35 (2): 319-330

5. Al-gubury, H. Y. and Q. Y. Mohammed. 2016. Prepared coupled ZnO–CO_2O_3 then study the photocatalytic activities using crystal violet dye, Journal of Chemical and Pharmaceutical Sciences, 9(3):1161-1165

6. Al-Qudah, M. A.; A. M. Saleh ; H. I.Al-Jaber; H. I. Tashtoush; J. N. Lahham ; M. H. Abu Zarga; F. U. Afifi and S. T. Abu Orabi. 2015. New isoflavones from *Gynandriris sisyrinchium* and their antioxidant and cytotoxic activities. Fitoterapia, 107: 15-21

7. Al-Qudah, M. A.; R. Muhaidat; I. N. Trawenhc; H. I. Al Jaberd; M. H. Abu Zargae and S. T. Abu orabia. 2012. Volatile constituents of leaves and bulbs of *Gynandriris sisyrinchium* and their antimicrobial activities. Jordan Journal of Chemistry. 7 (3):287-295.

8. Altameme H. J. M. 2018. Phytochemical Analysis of *Frankenia Aucheri* Jaub. Et Spach (Frankeniaceae) By GC-MS and FT-IR Techniques. Plant Archives 18 (2): 2263-2269

9. Altameme, H. J. M. 2016. GC-MS and FTIR analysis Phytocomponents on different parts of *Capparis spinosa* L. (Capparidaceae) in Iraq. Journal of Chemical and Pharmaceutical Sciences 9(4): 3269-3282

10. Altameme, H. J. M and I. A. Ibraheam, 2019. RAPD and ISSR analysis of the genetic relationship among some species in Rutaceae and Apiceae in Iraq. Iraqi Journal of Agricultural Sciences, 2(50): 608-616

11. El Shabrawy, M. O.A.; M. M. Marzouk; S. A. Kawashty; H. A. Hosni; I. A. El Garf and N.A.M. Saleh. 2013. Flavonoids from *Moraea sisyrinchium* (L.) Ker Gawl. (Iridaceae) in Egypt. International Conference on Applied Life Sciences (ICALS2013), UAE. September:15-17

12. Hameed, I. H.; H. J. Altameme and S. A. Idan. 2016. *Artemisia annua*: Biochemical products analysis of methanolic aerial parts extract and anti-microbial capacity. Research Journal of Pharmaceutical, Biological and Chemical Sciences**,**7(2): 1843-1868.

13. Harborne, J. B. 1984. Phytochemical Methods: A Guide to Modern Technique of Plant Analysis. 2nd. ed. Chapman and Hall. London, UK. PP:286

14. Jasim, H.; A.M. Hussein; I.H. Hameed and M.A. Kareem. 2015. Characterization of alkaloid constitution and evaluation of antimicrobial activity of *Solanum nigrum* by using (GC-MS), Journal of Pharmacognosy and Phytotherapy, 7(4):56-72

15. Mahadwad, O.K.; P.A. Parikh; R.V. Jasra and C. Patil. 2012. Photocatalytic degradation of reactive black-5 dye using TiO2-impregnated activated carbon, Environmental Technology, 33(3): 307–312

16. Rajesh J. Tayadea; K. S. Praveen; G. K. Ramchandra and V. J. Raksh 2007. Photocatalytic degradation of dyes and organic contaminants in water using nanocrystalline anatase and rutile TiO2, Science and Technology of Advanced Materials ,8: 455–462

17. Rokhsareh, S. S.; M. Maryam and N. Nasiri 2016. Synthesis, characterization and application of Lanthanide metal-ion-doped TiO_2 bentonite nanocomposite for removal of Lead (II) and Cadmium (II) from aquatic media, J. Water Environ. Nanotechnology., 1(1): 35-44

18. Sohrabi, M.R. and M. Ghavami. 2008. Photocatalytic degradation of Direct Red 23 dye using UV/TiO2: Effect of operational parameters, Journal of Hazardous Materials,153: 1235–1239

19. Townsend C.C. and E. Guest. 1985. Flora of Iraq, Vol. 8, Baghdad: Ministry of Agriculture and agrarian reform republic of Iraq pp: 232-235

20. Wahyuni S.; E. A. Saati; S. Winarsih ; E. Susetyarini and T.W. Rochmah. 2020. the combination of dragon fruits skin and teak leaves anthocyanin extract as soymilk's natural dye. Iraqi Journal of Agricultural Sciences, 51(4), 1188-1194.

21. Yang, J.; J. Dai; J. Zhao; and J. Miao. 2010. Mechanism of photocatalytic degradation of dye MG by TiO2-film electrode with cathodic bias potential, Chinese Sci Bull,.55 (2):201-211

22. Zeki, S. L. and M.J. M-Ridha, 2020. Phytoremediation of synthetic wastewater containing copper by using native plant. Iraqi Journal of Agricultural Sciences, 51(6), 1160-1612.